Hindawi
Mathematical Problems in Engineering
Volume 2021, Article ID 7136846, 12 pages
https://doi.org/10.1155/2021/7136846

Research Article

Continuum Damage Mechanics Approach for Modeling Cumulative-Damage Model

Haoran Li,[1] **Jiadong Wang**,[1] **Juncheng Wang**,[1] **Ming Hu**,[1] **and Yan Peng**[2]

[1]*Faculty of Mechanical Engineering and Automation, Zhejiang Sci-Tech University, Hangzhou 310018, China*
[2]*School of Mechanical Engineering, Yanshan University, Qinhuangdao 066004, China*

Correspondence should be addressed to Haoran Li; lihaoranysu@163.com

Received 10 April 2021; Revised 28 April 2021; Accepted 15 May 2021; Published 2 June 2021

Academic Editor: José António Fonseca de Oliveira Correia

In this study, we propose a novel cumulative-damage model based on continuum damage mechanics under situations where the mechanical components are subjected to variable loading. The equivalent completely reversed stress amplitude accounting for the effect of mean stress, stress gradients, loading history, and additional hardening behavior related to nonproportional loading paths on high-cycle fatigue under variable loading is elaborated. The effect of mean stress, stress gradients, loading history, and additional hardening behavior related to nonproportional loading paths is considered by averaging the superior limit of the intrinsic damage dissipation work in the critical domain. We developed a novel cumulative-damage model by introducing the equivalent completely reversed stress amplitude into the damage-evolution model. For better comparison, existing cumulative-damage models, including the Palmgren–Miner law, corrected Palmgren–Miner law, Morrow's plastic work interaction rule, and Wang's rule, were employed to predict the fatigue life under variable loading. The proposed model performed better, considering the error scatter band obtained by plotting the predicted and experimental fatigue life on the same coordinate system. The model precisely predicts fatigue life under variable loading and easily identifies its material constants.

1. Introduction

Fatigue failure should be considered in the engineering design to ensure safety and reliability during service life [1]. Fatigue failure assessment plays an important role in the design of engineering structures since it ensures the safety of engineering structures during their service lives. Since its initiation by Wohler in 1860, despite enormous efforts, reliable and consistent fatigue models applicable to complex loading history are still under development [2]. Substantial engineering structures in the industry fail by fatigue.

Engineering structures in the industry are usually subjected to variable loading. Variable loading, including variable amplitude and loading paths, is related to the fatigue life of engineering structures. Comparing the fatigue on constant loading, the fatigue on variable loading is always additionally investigated for the interactive effect associated with two adjacent load steps on fatigue life. For constant-amplitude and path loading, several researchers have proposed various fatigue criteria and described the effect of additional hardening behavior related to nonproportional loading paths [3], mean stress [4], and stress gradients [5, 6] on high-cycle fatigue. In general, those approaches can be roughly categorized into three, namely, strain energy method [7], critical plane approach [8, 9], stress-field intensity [10]. Stress gradients, well known as a factor affecting fatigue strength of metals, can be predicted by the theory of stress-field intensity since it was initially proposed aiming to the damage domain. Qylafku [11], Taylor [12], and Zeng [13] employed the stress-field intensity concept to model several fatigue criteria. Despite the significant efforts made on stress-field intensity methods, there is no general consensus as to the suitability of various loading situations, e.g., nonproportional loading. For high-cycle fatigue under variable loading, it has been reported that loading history significantly affects fatigue life, and several damage-accumulation models have been proposed. Despite the significant efforts made on damage-accumulation models, none has

gained widespread acceptance. Among them, Miner's damage-accumulation rule remains the most commonly adopted in practice [14]. Zhao [15] proposed a corrected Miner's damage-accumulation rule to improve the accuracy of prediction, while life predictions' accuracy has still been found unsatisfactory [16]. Drawbacks associated with the rules include their inability to express definite effects of the loading sequence on fatigue life [17]. Some other researchers, including Morrow et al. [18], Wang et al. [19], and Zhu et al. [20] established damage-accumulation models aiming at definite effects. Wang's rule was validated by multiaxial variable loading tests. Notably, damage parameters and fatigue life under constant-amplitude loading were employed to model Morrow's plastic work interaction rule and Wang's rule. Zhu et al. focused on isodamage lines-based methods and proposed a new nonlinear fatigue damage-accumulation model. Nevertheless, Xia et al. [21] reported that either damage parameter or fatigue life under constant-amplitude loading cannot reveal the definite effect of the loading sequence on fatigue life.

Initiated by Kachanov in 1958, continuum damage mechanics has been employed in modeling cumulative-damage models. Shang et al. [22], Hua et al. [23], and Yuan [24] proposed cumulative-damage models based on the damage-evolution model proposed by Lemaitre, which predicts the life expectancy of engineering structures subjected to variable loading. However, many material parameters in these models have to be identified, making them inconvenient for applications.

Here, we propose a new accumulative-damage model based on continuum damage mechanics, to improve the abovementioned shortcomings. First, the equivalent completely reversed stress amplitude, which accounts for the effect of additional hardening behavior related to nonproportional loading paths, mean stress, stress gradients, and loading history on high-cycle fatigue under variable loading, is elaborated using the stress-field intensity concept. The effect of loading history on fatigue life is established by combing damage parameters and fatigue life under constant-amplitude loading. Here, the equivalent completely reversed stress amplitude under single-stage loading is called the damage parameters. By introducing equivalent completely reversed stress amplitudes into the damage-evolution model, a new cumulative-damage model is established. The obtained rule compares very well with experimental data in the literature, and it is consistent with the previously proposed models, including the Palmgren–Miner law [17], corrected Palmgren–Miner law [15], Morrow's plastic work interaction rule [18], and Wang's rule [19]. Moreover, only one parameter is evaluated in our model, and it is very simple to obtain the model parameter.

2. Equivalent Completely Reversed Stress Amplitude

High-cycle fatigue failure is a local phenomenon, and the locality, also called the critical domain, is taken as a research object in stress-field intensity concepts. Nevertheless, the application of stress-field intensity concepts in investigating multiaxial high-cycle fatigue, especially under nonproportional loading, has not been extensively studied. Here, we propose damage parameters, based on continuum damage mechanics and stress-field intensity concepts, to model the cumulative-damage model.

Continuum damage mechanics has provided a method for analyzing damage development by introducing a damage variable into the constitutive stress-strain relationship. As one of the outstanding examples, Lemaitre et al. [25] proposed a differential equation for damage development. Distinguishingly, the damage development equation can be expressed as follows for the components subjected to fully reversed tension:

$$\frac{\mathrm{d}D}{\mathrm{d}N} = \frac{\eta \sigma_{-1a}^{2p+2}}{(1-D)^{2p+2}}. \tag{1}$$

To develop the damage development equation available for multiaxial high-cycle fatigue, equation (1) is modified as follows:

$$\frac{\mathrm{d}D}{\mathrm{d}N} = \frac{\eta (1 - cr - cr\sin\theta)\sigma_{\mathrm{eq}a}^{2p+2}}{(1-D)^{2p+2}}, \tag{2}$$

where $\sigma_{\mathrm{eq}a}$ is the damage parameter describing the effect of additional hardening behavior related to nonproportional loading paths and mean stress on high-cycle fatigue under single-stage constant loading. The damage parameter is expressed as equation (3), as proposed by Freitas et al. [26]. The parameter c proposed by Yao et al. [27], which is employed when considering the effect of stress gradients, is also utilized here, and it is expressed as equation (4). Considering the variety of c under situations where the mechanical component is subjected to nonproportional loading, c is calculated when $\sigma_{\mathrm{eq,\,max}}$ reaches the maximum value. Certainly,

$$\sigma_{\mathrm{eq}a} = \frac{f_{-1}}{\tau_{-1}}\sqrt{\frac{\sigma_a^2}{3} + \tau_a^2} + \left(3 - \frac{\sqrt{3}\, f_{-1}}{\tau_{-1}}\right)\sigma_{H\max}, \tag{3}$$

$$c = \left|\frac{1}{\max\left[\sigma_{\mathrm{eq,\,max}}(t)\right]}\frac{\mathrm{d}\sigma_{\mathrm{eq}}}{\mathrm{d}r}\right|, \tag{4}$$

the damage evolution equation can also be obtained from the explicit expression of damage variables as follows:

$$D = 1 - \left[1 - \frac{N_{-1f}}{N_f}\right]^{(1/2p+3)}, \tag{5}$$

where N_f is the fatigue life of a point located at the critical domain and N_{-1f} is the predicted life equivalent to that of structural components subjected to fully reversed tensile loading. Both are, respectively, expressed as follows:

$$N_f = \frac{M\sigma_{\mathrm{eq}a}^{-(2p+2)}}{(2p+3)(1 - cr - cr\sin\theta)}\left[1 - (1 - D_c)^{2p+3}\right], \tag{6}$$

$$N_{-1f} = \frac{M\sigma_{-1a}^{-(2p+2)}}{2p+3}\left[1 - (1 - D_c)^{2p+3}\right]. \tag{7}$$

Introducing stress-field intensity concepts, the average superior limit of the intrinsic damage dissipation work [28] in the critical domain can be obtained as the left side of equation (8). The hypothetical condition that the same average superior limit of the intrinsic damage dissipation work in the critical domain implies the same fatigue life is captured to formulate the damage parameters in our model. To simplify, the average superior limit of the intrinsic damage dissipation work in the critical domain for smooth structural components subjected to fully reversed tensile loading can be obtained as the right side of the following equation:

$$\frac{1}{V}\int_V\left(\int_0^D Y_{\max}\mathrm{d}D\right)\mathrm{d}V=\int_0^{D_c}\frac{\sigma_{-1\mathrm{eq}a}^2}{2E(1-D)^2}\mathrm{d}D. \tag{8}$$

Then, expanding equation (8), the following equation is obtained:

$$\begin{cases}\dfrac{1}{V}\displaystyle\int_V\left[\frac{\langle\sigma_{\mathrm{eq}}^2R_\gamma\rangle_{\max}}{2E(1-D)}-\frac{\langle\sigma_{\mathrm{eq}}^2R_\gamma\rangle_{\max}}{2E}\right]\mathrm{d}V=\frac{\sigma_{-1\mathrm{eq}a}^2}{2E(1-D_c)}-\frac{\sigma_{-1\mathrm{eq}a}^2}{2E},\\[2ex] R_\gamma=\dfrac{2(1+\nu)}{3}+3(1-2\nu)\left(\dfrac{\sigma_H}{\sigma_{\mathrm{eq}}}\right)^2.\end{cases} \tag{9}$$

Substituting equations (5)–(7) into equation (9) and employing first-order approximation, the damage parameters are finally expressed as follows. Notably, several material constants are contracted to consider the self-consistency of the damage parameters:

$$\sigma_{-1\mathrm{eq}a}=\left\{\frac{1}{V}\int_V\left[\sigma_{\mathrm{eq}a}^{2p+2}\langle\sigma_{\mathrm{eq}}^2R_\gamma\rangle_{\max}(1-cr-cr\sin\theta)\right]\mathrm{d}V\right\}^{1/2p+4}. \tag{10}$$

Numerous fatigue experiments of variable amplitude have shown that loading history has a remarkable effect on fatigue life. For structural components subjected to uniaxial loading, different loading sequence makes Miner's cumulative critical value fall in different regions. When structural components are subjected to a high-low loading sequence, Miner's cumulative critical value falls below one, and conversely, for a low-high loading sequence, the value is greater than one. Here, by combing the damage parameters, the equivalent completely reversed stress amplitude considering the loading sequence is proposed as follows:

$$\begin{cases}\sigma_{-1mseqa,i}=\sigma_{-1\mathrm{eq}a,i}\left(\dfrac{n_{i-1}}{N_{fi-1}}\right)^{(1/2p+2)-(1/2p+2)\phi_i}, & (i\geq 2),\\[2ex] \phi_i=\left[\dfrac{\mathrm{In}\left(\sigma_{-1\mathrm{eq}a,i}-\sigma_{-1}\right)\mathrm{In}N_{fi-1}}{\mathrm{In}\left(\sigma_{-1\mathrm{eq}a,i-1}-\sigma_{-1}\right)\mathrm{In}N_{fi}}\right]^{p+1},\end{cases} \tag{11}$$

where ϕ_i is the contraction towards the partial variables in equation (11).

3. Proposed Cumulative-Damage Model

For smooth structural components subjected to single-stage fully reversed tensile loading, the damage-evolution equation can be obtained from the explicit expression of the damage variable:

$$\begin{cases}D=1-\left[1-\dfrac{n_{-1}}{N_{-1f}}\right]^{1/2p+3},\\[2ex] N_{-1f}=\dfrac{M\sigma_{-1a}^{-(2p+2)}}{2p+3}\left[1-\left(1-D_c\right)^{2p+3}\right].\end{cases} \tag{12}$$

Substituting equation (11) into (12), the expression of the damage-evolution associated with ith loading step can be obtained as follows:

$$D_i=1-\left[1-\left(\frac{n_{i-1}}{N_{fi-1}}\right)^{1-\phi_i}\frac{n_i}{N_{fi}}\right]^{1/2p+3},\quad (i\geq 2). \tag{13}$$

Then, the expression of damage-evolution associated with the first loading step (equation (13)) should be rewritten as follows:

$$D_1=1-\left(1-\frac{n_1}{N_{f1}}\right)^{1/2p+3}. \tag{14}$$

For structural components subjected to two-step loading, the expression of damage-evolution associated with the second loading step can be expressed as follows:

$$D_2=1-\left[1-\left(\frac{n_1}{N_{f1}}\right)^{1-\phi_2}\frac{n_2}{N_{f2}}\right]^{1/2p+3}. \tag{15}$$

Based on the damage-equivalent concepts [19], if the fatigue life and applied cycles under $i-1^{\mathrm{th}}$ constant-amplitude loading are N_{f1-1} and n_{i-1}, then the damage caused by n_{i-1} cycle loading can be equivalent to that caused by n_i' cycle loading at the ith level, i.e., $D_i'=D_{i-1}$. Then, the equivalent damage of the first loading step can be obtained through the second loading step by combining equations (14) and (15). The equivalent relation can be expressed as follows:

$$\frac{n_2'}{N_{f2}}=\left(\frac{n_1}{N_{f1}}\right)^{\phi_2}. \tag{16}$$

Applying the superposable fatigue-life condition to a single-loading step, $N_{f2}=n_2'+n_2$, and the cumulative-damage model for two steps loading can be established as follows:

$$\left(\frac{n_1}{N_{f1}}\right)^{\phi_2}+\frac{n_2}{N_{f2}}=1. \tag{17}$$

Distinguishingly, the cumulative-damage rule for structural components is subjected to two-step uniaxial loading (fully reversed tensile loading), and we conclude that different loading sequence makes Miner's accumulative

critical value fall in different regions. The principle associated with the conclusion is expressed in equation (18). For structural components subjected to high-low two-step uniaxial loading (fully reversed tensile loading), Miner's cumulative critical value falls below one, and conversely, the sum is greater than one:

$$\begin{cases} \dfrac{n_1}{N_{f1}} + \dfrac{n_2}{N_{f2}} \geq \left(\dfrac{n_1}{N_{f1}}\right)^{\phi_2} + \dfrac{n_2}{N_{f2}} = 1, \quad \left(\sigma_{a2} \geq \sigma_{a1}, N_{f1} \geq N_{f2}\right), \\ \dfrac{n_1}{N_{f1}} + \dfrac{n_2}{N_{f2}} < \left(\dfrac{n_1}{N_{f1}}\right)^{\phi_2} + \dfrac{n_2}{N_{f2}} = 1, \quad \left(\sigma_{a2} < \sigma_{a1}, N_{f1} < N_{f2}\right). \end{cases} \tag{18}$$

Furthermore, for structural components subjected to three-step loading, the expression of damage-evolution associated with the third loading step can be expressed as equation (19), and it is obtained from equation (13). The damage-evolution associated with the second loading step can be obtained from equation (15), and it is explicitly expressed in equation (20):

$$D_3 = 1 - \left[1 - \left(\frac{n_2}{N_{f2}}\right)^{1-\phi_3} \frac{n_3}{N_{f3}}\right]^{1/2p+3}, \tag{19}$$

$$D_2 = 1 - \left[1 - \left(\frac{n_1}{N_{f1}}\right)^{1-\phi_2} \left(\frac{n_2}{N_{f2}} + \frac{n_2'}{N_{f2}}\right)\right]^{1/2p+3}. \tag{20}$$

Then, one can obtain the cumulative-damage model for three-step loading based on the damage-equivalent concepts. The resulting cumulative-damage model for three-step loading is expressed as follows:

$$\left(\frac{n_1}{N_{f1}}\right)^{1-\phi_2} \left\{\left(\frac{n_2}{N_{f2}}\right)^{\phi_3} + \frac{n_2'}{N_{f2}} \left(\frac{n_2}{N_{f2}}\right)^{\phi_3 - 1}\right\} + \frac{n_3}{N_{f3}} = 1. \tag{21}$$

Similarly, the recurrence formula of the ith level loading can be expressed as follows:

$$\begin{cases} \dfrac{n_i'}{N_{fi}} + \dfrac{n_i}{N_{fi}} = 1, \quad (i \geq 3), \\ \left(\dfrac{n_{i-2}}{N_{fi-2}}\right)^{1-\phi_{i-1}} \left\{\left(\dfrac{n_{i-1}}{N_{fi-1}}\right)^{\phi_i} + \dfrac{n_{i-1}'}{N_{fi-1}} \left(\dfrac{n_{i-1}}{N_{fi-1}}\right)^{\phi_i - 1}\right\} = \dfrac{n_i'}{N_{fi}}, \\ \dfrac{n_2'}{N_{f2}} = \left(\dfrac{n_1}{N_{f1}}\right)^{\phi_2}. \end{cases} \tag{22}$$

The application of the new cumulative-damage model for predicting the fatigue life of structural components under variable loading involves identifying the material parameter p. Material parameter p can be obtained by analyzing the experimental data associated with a specimen subjected to fully reversed tensile loading employing the least square method. Certainly, the resulting identification model (equation (23)) is derived by combing equation (12) and the least-square method:

$$p = \frac{\sum_{i=1}^{j} \lg N_{-1f,i} \sum_{i=1}^{j} \lg \sigma_{-1a,i} - j \sum_{i=1}^{j} \lg N_{-1f,i} \lg \sigma_{-1a,i}}{2j \sum_{i=1}^{j} \left(\lg \sigma_{-1a,i}\right)^2 - 2\left(\sum_{i=1}^{j} \lg \sigma_{-1a,i}\right)^2} - 1. \tag{23}$$

4. Evaluation by the Experimental Data

4.1. Uniaxial Loading Condition. The uniaxial two-level step-loading test data for C35, SAE4130, and 7050-T7451 (Table 1) were used to evaluate the proposed damage-cumulative model. For better comparison, existing popular cumulative-damage models, including Palmgren–Miner law, corrected Palmgren–Miner law, and Wang's rule, were employed to predict the fatigue life under the loading conditions. All experimental data and material parameters required in these models are listed in Table 2.

For better comparison, the total fatigue life under uniaxial two-level step loading and that predicted using the Palmgren–Miner law, corrected Palmgren–Miner law, Wang's rule, and the proposed model are plotted on the same coordinate plane (Figure 1). 97.8% of the predicted data fall within an error factor of 2, and the proportion for the data predicted by the other models is 78.2%, 80.4%, and 82.6% for Palmgren–Miner law, corrected Palmgren–Miner law, and Wang's rule, respectively. To predict fatigue life for uniaxial two-level loading, the proposed model yielded better results than other tested models.

4.2. Multiaxial Loading Condition. To evaluate the proposed model for predicting structural components under multiaxial variable loading, multiaxial two-level and two-stage block-loading test data for LY12CZ (Table 3) were used. The cylindrical specimens were subjected to combined torsion and tension. First, the equivalent completely reversed stress amplitude in the specimen under the stress condition was evaluated. Then, the proposed cumulative-damage model was employed to predict the fatigue life of the cylindrical specimen under multiaxial variable loading.

Considering the cylindrical specimen subjected to combined torsion and tension, at each point located in the critical domain of the specimen, we define the coordinate system (Figure 2). In this frame, the stress state under combined torsion and tension is described by the following components and aimed at each point located in the critical domain:

Table 1: Uniaxial two-level step-loading test data and predicted life using the tested rules [29, 30].

Materials	σ_{a1}	σ_{a2}	n_1/N_{f1}	Min.	C. Miner	Wan.	Pro.	Exp.
C35	353	275	0.1	689200	461200	645282	181625	353280
C35	353	275	0.25	583000	355000	522964	124743	226560
C35	353	275	0.5	406000	178000	350078	84092	108840
C35	353	275	0.75	229000	1000	195578	63672	80040
C35	334	275	0.1	695000	467000	665427	282970	425960
C35	334	275	0.25	597500	369500	555925	205401	209140
C35	334	275	0.5	435000	207000	395480	149872	203200
C35	334	275	0.75	272500	44500	248607	123416	141780
C35	353	294	0.1	365200	245200	347626	159006	218400
C35	353	294	0.25	313000	193000	288484	114354	200600
C35	353	294	0.5	226000	106000	202826	80373	129200
C35	353	294	0.75	139000	19000	125034	62535	80600
C35	334	294	0.1	371000	251000	360633	233743	245800
C35	334	294	0.25	327500	207500	312617	182448	214300
C35	334	294	0.5	255000	135000	240633	141918	173000
C35	334	294	0.75	182500	62500	173737	121174	137700
C35	275	353	0.1	122800	107200	125055	128000	134240
C35	275	353	0.25	229000	213400	232769	242000	243560
C35	275	353	0.75	583000	567400	585675	617765	614200
C35	294	334	0.1	139000	106000	141485	149837	156600
C35	294	334	0.25	182500	149500	186429	207822	205600
C35	294	334	0.75	327500	294500	330098	361257	385800
SAE4130	648	552	0.25	224875	140275	210665	110429	92617
SAE4130	648	552	0.5	167750	83150	154192	80376	57488
SAE4130	648	552	0.75	110625	26025	102410	63762	55353
SAE4130	607	552	0.25	239000	154400	231274	168434	94898
SAE4130	607	552	0.5	196000	111400	188474	137549	109990
SAE4130	607	552	0.75	153000	68400	148386	120257	104496
SAE4130	648	565	0.25	181375	114175	171584	101796	118431
SAE4130	648	565	0.5	138750	71550	129353	76481	84542
SAE4130	648	565	0.75	96125	28925	90412	62289	63421
SAE4130	607	565	0.25	195500	128300	190834	153281	132108
SAE4130	607	565	0.5	167000	99800	162428	130673	121080
SAE4130	607	565	0.75	138500	71300	135687	117725	113412
7050	176	133	0.074	58856	40436	57885	55929	54852
7050	176	133	0.148	56312	37892	54924	52311	58708
7050	176	133	0.5	44213	25793	42588	39868	30449
7050	176	133	0.741	35929	17509	34903	33249	37627
7050	176	85	0.074	211090	143350	201638	176399	274446
7050	176	85	0.148	196381	128641	183362	153578	204383
7050	176	85	0.741	78509	10769	69646	55401	92428
7050	176	85	0.395	147284	79544	131814	103301	80475
7050	133	85	0.082	212319	144579	206720	191883	200205
7050	133	85	0.164	198838	131098	191046	172476	244318
7050	133	85	0.821	90827	23087	86925	79630	216409
7050	133	85	0.5	143600	75860	135023	117757	68700

Note: Min.: Palmgren–Miner damage cumulative law, C. Miner: corrected Palmgren–Miner damage cumulative law, Wan.: Wang YY's damage cumulative law, Pro.: our proposal, Exp.: median fatigue experimental life, 7050-7050-T7451 aluminum alloy.

$$\begin{cases} \sigma\left(r_D, \theta, t\right) = \sigma_a \sin \omega t + \sigma_m = \sigma\left(t\right), \\ \tau\left(r_D, \theta, t\right) = \left[\tau_a \sin\left(\omega t - \delta\right) + \tau_m\right] \sqrt{1 + \dfrac{r_D^2}{R^2} - \dfrac{2 r_D \cos\theta}{R}} = \tau\left(t\right) \sqrt{1 + \dfrac{r_D^2}{R^2} - \dfrac{2 r_D \cos\theta}{R}}. \end{cases} \tag{24}$$

Table 2: Experimental data and material parameters required in predicted models [29, 30].

Materials	$\sigma_{-1a,1}$	$N_{-1f,1}$	$\sigma_{-1a,2}$	$N_{-1f,2}$	$\sigma_{-1a,3}$	$N_{-1f,3}$	$\sigma_{-1a,4}$	$N_{-1f,4}$	σ_{-1}	p
C35	353	52000	334	110000	294	400000	275	760000	216	4.30
SAE4130	648	53500	607	110000	565	224000	552	282000	391	4.17
7050-T7451	176	27027	133	61400	85	225800	- -	- -	23	0.46

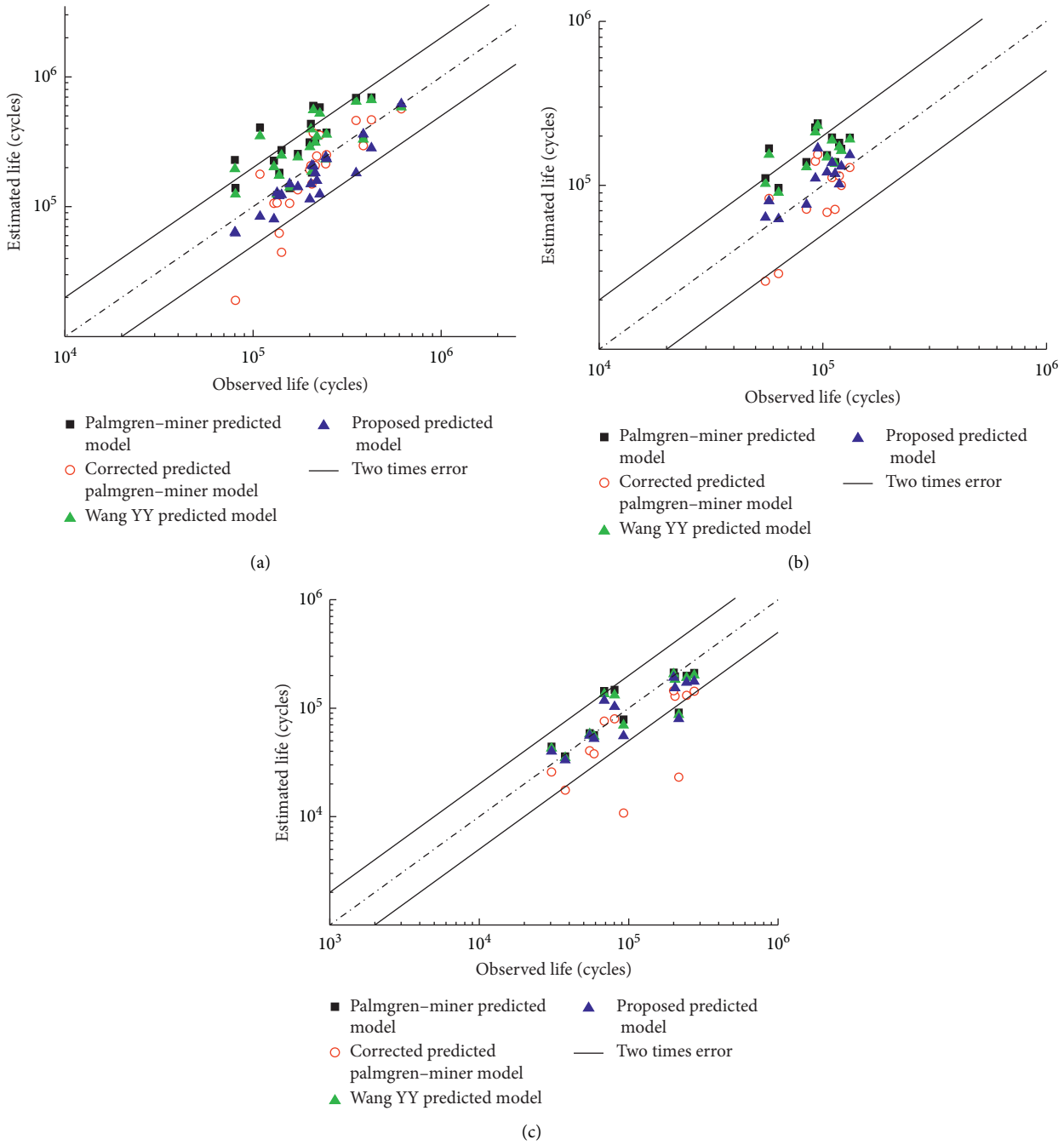

Figure 1: Assessment for the proposed model by means of three kinds of materials. (a) Fatigue life predictions using test models for C35 under two-level step loading. (b) Fatigue life predictions using test models for SAE4130 under two-level step loading. (c) Fatigue life predictions using test models for 7050-T7451 under two-level step loading.

Table 3: Total predicted fatigue life of LY12CZ under multiaxial two-level and two-stage block loading [21, 31].

No.	Loading paths	n_1/N_{f1}	$[n/N_f]_i$	Min.	Mor.	Wan.	Pro.	Exp.
1	$C_1 \longrightarrow C_2$	0.5	-	48376	42383	37075	19738	19149
2	$C_2 \longrightarrow C_1$	0.5	-	48376	47476	50023	53128	51304
3	$C_2 \longrightarrow C_1$	0.25	-	29721	29271	31124	32433	28888
4	$A_1 \longrightarrow A_2$	0.5	-	197263	170789	162735	64582	74635
5	$A_2 \longrightarrow A_1$	0.5	-	197263	195890	198935	204827	196934
6	$B_1 \longrightarrow B_2$	0.5	-	179564	155162	141583	49528	63348
7	$B_2 \longrightarrow B_1$	0.5	-	179564	178732	180794	184378	184835
8	$A_1 \longrightarrow C_1$	0.5	-	13949	13908	17421	14084	11811
9	$C_1 \longrightarrow A_1$	0.5	-	13949	13887	9718	13747	9357
10	$A_1 \longrightarrow B_1$	0.18	-	11394	11381	11667	11815	5236
11	$A_2 \longrightarrow A_3$	0.5	-	68212	67776	68833	72565	132923
12	$A_3 \longrightarrow A_2$	0.5	-	68212	67602	67336	62414	75311
13	$B_1 \longrightarrow C_3$	0.5	-	6872	6865	8379	7252	6104
14	$C_3 \longrightarrow B_1$	0.5	-	7991	7969	4684	7166	4673
15	$C_3 \longrightarrow B_3$	0.4	-	36056	32048	15406	15135	24138
16	$A_2 \longrightarrow A_4$	0.5	-	77703	74935	77846	68579	111423
17	$A_4 \longrightarrow A_2$	0.5	-	77703	71814	77550	88552	98732
18	$A_3 \longrightarrow A_5$	0.4	-	27873	27674	28477	30466	39078
19	$A_5 \longrightarrow A_3$	0.4	-	37354	35565	33592	21323	16875
20	$B_3 \longrightarrow C_3$	0.4	-	25582	25039	27225	27240	29967
21	$A_5 \longrightarrow A_6$	0.5	-	20318	19910	20729	20901	20619
22	$A_6 \longrightarrow A_5$	0.5	-	20318	18721	18912	18356	22650
23	$[A_1 \longrightarrow C_1]$	-	$[0.06]_1, [0.09]_2$	13042	13430	12112	12000	8746
24	$[A_6 \longrightarrow A_5]$	-	$[0.03]_1, [0.11]_2$	13106	13130	13916	8000	11986
25	$[A_5 \longrightarrow A_6]$	-	$[0.11]_1, [0.03]_2$	13025	12565	14052	9000	18052

Note: $[x \longrightarrow y]$: single program sequence including loading paths; $[n/N_f]_i$: each life score for single program sequence.

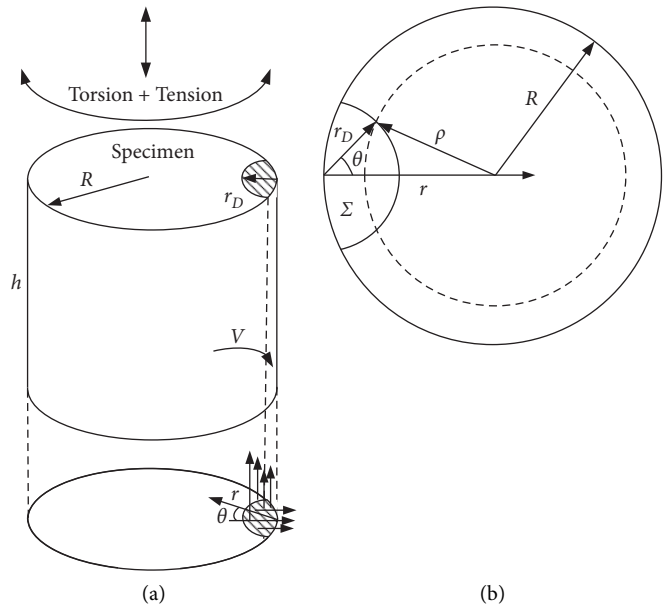

Figure 2: Distribution of the critical damage domain of a smooth specimen in multiaxial stress states for combined torsion and tension.

Then, von Mises equivalent stress is expressed as follows (equation (24)):

$$\sigma_{\mathrm{eq}}(r_D, \theta, t) = \sqrt{\sigma^2(t) + 3\tau^2(t)\left(1 + \frac{r_D^2}{R^2} - \frac{2r_D\cos\theta}{R}\right)}. \tag{25}$$

Considering $r_D \ll R$, the following approximate equation for equation (25) is established:

$$\sigma_{\mathrm{eq}}(r_D, \theta, t) \approx \sigma_{\mathrm{eq}}(0, 0, t) = \sqrt{\sigma^2(t) + 3\tau^2(t)}. \tag{26}$$

Substituting equation (26) into (4), the coefficient c will be zero, which expresses the effect of the stress gradient on

fatigue life. Based on the same approximate principle, the following approximate equations are established:

$$\sigma_{\mathrm{eq}\,a}(r_D,\theta) \approx \frac{f_{-1}}{\tau_{-1}}\sqrt{\frac{\sigma_a^2}{3}+\tau_a^2}+\left(1-\frac{\sqrt{3}\,f_{-1}}{3\tau_{-1}}\right)(\sigma_a+\sigma_m), \tag{27}$$

$$\langle\sigma_{\mathrm{eq}}^2(r_D,\theta,t)R_\gamma(r_D,\theta,t)\rangle_{\max} \approx \max\left[\frac{2(1+\nu)}{3}\sigma_{\mathrm{eq}}^2(0,0,t)+3(1-2\nu)\sigma_m^2(t)\right]. \tag{28}$$

Ultimately, the equivalent completely reversed stress amplitude for the cylindrical specimen subjected to combined torsion and tension can be obtained by substituting equations (26)–(28) into equation (10):

$$\sigma_{-1\mathrm{eq}a}=\left[\langle\sigma_{\mathrm{eq}}^2R_\gamma\rangle_{\max}\right]^{1/2p+4}\left[\frac{\sigma_{-1}}{\tau_{-1}}\sqrt{\frac{\sigma_a^2}{3}+\tau_a^2}+\left(1-\frac{\sqrt{3}\,\sigma_{-1}}{3\tau_{-1}}\right)(\sigma_a+\sigma_m)\right]^{(2p+2/2p+4)},\quad(\sigma_a\neq 0). \tag{29}$$

Note that equation (29) cannot be applied in the case of pure torsion since a large error is obtained by making $c=0$. However, one can immediately establish the equivalent relationship between the endurance limits under fully reversed tension and torsion from equation (10):

$$\sigma_{-1}=\tau_{-1}\left\{\frac{1}{V}\int_V\left[\left(\frac{\sigma_{-1}}{\tau_{-1}}\right)^{2p+2}[f(r_D)]^{2p+4}2(1+\nu)(1-cr-cr\sin\theta)\right]\mathrm{d}V\right\}^{1/2p+4}. \tag{30}$$

Analogously, the following equation for expressing the equivalent completely reversed stress amplitude under pure torsion can be obtained:

$$\sigma_{-1\mathrm{eq}a}=\tau_a^{p+1/p+2}(\tau_a+\tau_m)^{1/p+2}\left\{\frac{1}{V}\int_V\left[\left(\frac{\sigma_{-1}}{\tau_{-1}}\right)^{2p+2}[f(r_D)]^{2p+4}2(1+\nu)(1-cr-cr\sin\theta)\right]\mathrm{d}V\right\}^{1/2p+4}. \tag{31}$$

A concise form of equation (31) can be obtained by introducing equation (30) into equation (31):

$$\sigma_{-1\mathrm{eq}a}=\frac{\sigma_{-1}}{\tau_{-1}}\tau_a^{p+1/p+2}(\tau_a+\tau_m)^{(1/p+2)}. \tag{32}$$

Therefore, the proposed cumulative-damage model for predicting the fatigue life of structural components under multiaxial two-level variable loading and combined torsion and tension can be explicitly expressed as follows:

$$\begin{cases} N_{\mathrm{predicted}}=\left\{1-\left(\dfrac{n_1}{N_{f1}}\right)^{\phi_2}\right\}N_{f2}+n_1, \\ \sigma_{-1\mathrm{eq}a,i}=\begin{cases}\left[\langle\sigma_{\mathrm{eq}i}^2R_{\gamma i}\rangle_{\max}\right]^{1/2p+4}\sigma_{\mathrm{eq}ai}^{2p+2/2p+4}, & (i=1,2 \text{ and } \sigma_{ai}\neq 0 \text{ or } \sigma_{mi}\neq 0), \\ \dfrac{\sigma_{-1}}{\tau_{-1}}\tau_{ai}^{p+1/p+2}(\tau_{ai}+\tau_{mi})^{1/p+2}, & (i=1,2 \text{ and } \sigma_{ai}=0,\ \sigma_{mi}=0).\end{cases}\end{cases} \tag{33}$$

Engineering structures are usually subjected to block program sequence loading. It is important to study certain fatigue issues, such as cumulative-damage under program sequence loading. Hence, we investigated cumulative-damage under multiaxial two-stage block loading and combined torsion and tension using the proposed model. Based on damage-equivalent concepts, the damage caused by n_{i-1} cycle loading is equivalent to that caused by n_i' cycle loading at the ith level. The variable Z_i expresses the ratio of the absorbed fatigue n_i' with the total fatigue life under single-stage loading, and its expression is derived from equations (22) and (33) as follows:

$$\begin{cases} \sigma_{-1\mathrm{eq}a,i} = \begin{cases} \left[\langle \sigma_{\mathrm{eq}i}^2 R_{\gamma i}\rangle_{\max}\right]^{1/2p+4} \sigma_{\mathrm{eq}ai}^{2p+2/2p+4}, & \begin{pmatrix} i=1,2 \text{ and } \sigma_{ai}\neq 0 \\ \text{or } \sigma_{mi}\neq 0 \end{pmatrix}, \\ \dfrac{\sigma_{-1}}{\tau_{-1}}\tau_{ai}^{p+1/p+2}\left(\tau_{ai}+\tau_{mi}\right)^{1/p+2}, & \begin{pmatrix} i=1,2 \text{ and} \\ \sigma_{ai}=0, \sigma_{mi}=0 \end{pmatrix}, \end{cases} \\ Z_2 = \left(\dfrac{n_1}{N_{f1}}\right)^{\phi_2}, \\ Z_i = \left(\dfrac{n_{i-2}}{N_{fi-2}}\right)^{1-\phi_{i-1}} \left\{ \left(\dfrac{n_{i-1}}{N_{fi-1}}\right)^{\phi_i} + Z_{i-1}\left(\dfrac{n_{i-1}}{N_{fi-1}}\right)^{\phi_i - 1} \right\}, \quad (i \geq 3). \end{cases} \tag{34}$$

For the fatigue-life prediction under program sequence loading, we may be ignorant of the level loading causing component failure, and consequently, Z_i cannot be calculated. However, the sequence of Z_i, i.e., $Z_2, Z_3, \ldots$, can be calculated from equation (34). According to the sequence of Z_i, component failure will result at the $i-1^{\text{th}}$ level due to fatigue once $Z_i \geq 1$. There may be two cases of cumulative-damage at $i-1^{\text{th}}$ level, even under at $Z_i \geq 1$. The predicted fatigue life for two cases can be, respectively, expressed as follows:

$$\begin{cases} N_{\text{predicted}} = \sum_{k=1}^{i-2} n_k + n_{i-1}, & \left(\text{if } Z_{i-1} + \dfrac{n_{i-1}}{N_{fi-1}} \leq 1\right), \\ N_{\text{predicted}} = \left(1 - Z_{i-1}\right) N_{fi-1} + \sum_{k=1}^{i-2} n_k, & \left(\text{if } Z_{i-1} + \dfrac{n_{i-1}}{N_{fi-1}} > 1\right). \end{cases} \tag{35}$$

The proposed model was assessed for predicting the fatigue life of structural components under multiaxial two-level and two-stage block loading and combined torsion and tension using relevant data for LY12CZ (Table 3). The proposed model for predicting fatigue life under two kinds of loading is expressed in equations (33) and (35). For better comparison with other cumulative-damage models, including the Palmgren–Miner law, Morrow's plastic work interaction rule, and Wang's rule, the models were synchronously used to predict the fatigue life of LY12CZ, and all text data under single-stage loadings and material parameter required in these models are listed in Tables 4 and 5. Notably, multiaxial equivalent stress parameters are employed in Morrow's plastic work interaction rule. However, in the proposed model, the equivalent stress parameters are replaced by Matake's critical plane stress parameters [32], and the interaction exponent is set to −0.45 [33].

The predicted fatigue life of LY12CZ under multiaxial two-level step and two-stage block loading based on the test cumulative-damage models is shown in Figure 3. The percentage of the predicted data falling within the factor of 2.05 scatter band is 80%, 80%, 88%, and 96% for the Palmgren–Miner law, Morrow's plastic work interaction rule, Wang's rule, and our model, respectively. For predicting the fatigue life of LY12CZ under multiaxial variable loading, including two-level step loading and two-stage block loading, our model yielded results comparable to those of the test cumulative-damage models.

Table 4: Test results under single-stage loadings for LY12CZ [21, 31].

Loading paths	σ_a	σ_m	τ_a	τ_m	δ	N_f	$\sigma_{-1\mathrm{eq}a}$	σ_{Matake}
A1	247.52	0	142.91	0	0	16831	333	242
A2	176.81	0	102.08	0	0	377694	238	173
A3	250	0	0	0	0	56316	250	179
A4	0	0	144.3	0	0	75299	204	146
A5	0	0	202.08	0	0	8911	285	202
A6	350	0	0	0	0	31725	350	250
B1	247.52	0	142.91	0	45	10229	326	246
B2	176.81	0	102.08	0	45	348899	234	176
B3	158	0	125	0	45	57004	246	188
C1	247.52	0	142.91	0	90	11067	308	246
C2	176.81	0	102.08	0	90	85684	220	176
C3	250	0	144.34	0	90	4634	312	248

Table 5: Material parameters required in the proposed model for LY12CZ [31].

Materials	σ_{a1}	N_{f1}	σ_{a2}	N_{f2}	σ_{a3}	N_{f3}	σ_{-1}	p
LY12CZ	350	31725	300	140670	250	272123	169	2.15

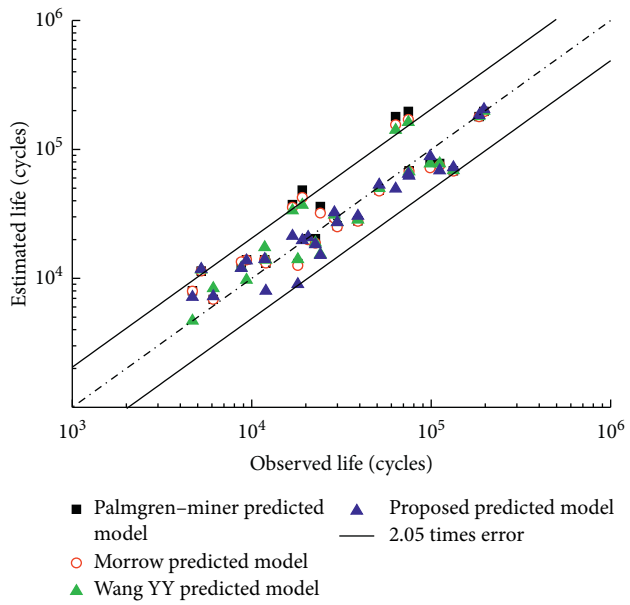

Figure 3: Fatigue life predictions for LY12CZ under multiaxial variable loading based on test damage cumulative models.

5. Conclusions

Here, we propose a cumulative-damage model based on continuum damage mechanics to evaluate the fatigue life of smooth structural components under axial and multiaxial variable loading. The conclusions can be obtained as follows:

(1) The model is very competitive with the existing test cumulative-damage models. It adopts a kind of equivalent completely reversed stress amplitude that expresses the effect of mean stress, stress gradients, loading history, and additional hardening behavior related to nonproportional loading paths on high-cycle fatigue under variable loading.

(2) Only one parameter is evaluated for the application of our model, and it is very simple to obtain the model parameter which is a simple function on the slope of S-N curve of materials.

(3) The concept of equivalent completely reversed stress amplitude provides a new conception to investigate the cumulative damage for structural components under variable loading. Cumulative damage during fatigue progress and fatigue life can be precisely predicted by combining the equivalent completely reversed stress amplitude and damage development equation.

Abbreviations

V: Volume of the critical domain
σ_{-1a}, $\sigma_{-1\mathrm{eq}a}$, and $\sigma_{-1m\mathrm{seq}a}$: Stress amplitude under fully reversed loading in tension, damage parameters, and equivalent completely reversed stress amplitude, respectively
D: Internal damage variable
$\sigma_{\mathrm{eq,max}}$: Maximum von Mises equivalent stress in the critical domain
r and θ: Polar diameter within polar coordinates and polar angle within polar coordinates, respectively
M and p: Material parameters dependent on the slope of S-N curve
$\sigma_{-1\mathrm{eq}a,i}$ and $\sigma_{-1m\mathrm{seq}a,i}$: Damage parameters for the ith level loading and equivalent completely reversed stress amplitude for the ith level loading, respectively

N_{fi} and n_{fi}: Fatigue life and applied cycles, respectively, under the ith level constant-amplitude loading
σ_{-1}: Endurance limits in reversed tension
n_{-1}: Applied cycles under fully reversed loading in tension
D_i: Internal damage variable of the ith step loading
D_i' and n_i': Equivalent internal damage variable and applied cycles, respectively, based on damage-equivalent concepts, respectively
σ_{ai}: ith level stress amplitude under fully reversed loading in tension
$\sigma_{-1a,i}$ and $N_{-1f,i}$: Stress amplitude and fatigue life plotted in S-N curve
σ_{Matake}: Damage parameters proposed by Matake et al.
E: Elastic modulus
σ_{eq}: von Mises equivalent stress
R_γ: Three axis factor
$\sigma_{H\max}$: Maximum hydrostatic stress in one cycle
$\langle\cdot\rangle_{\max}$: Maximum value in symbol
$Y_{\max}$: Maximum generalized force of damage driving in one cycle
ν: Poisson ratio
σ_H: Hydrostatic stress
$f(r_D)$: Stress distribution function in the critical domain
$N_{\text{predicted}}$: Predicted life of smooth specimen
D_c: The critical value of damage
$\sigma_a, \sigma_m, \tau_a$, and τ_m: Normal stress amplitude, normal mean stress, shear stress amplitude, and shear mean stress, respectively
δ: Phase difference between normal loading path and shear-loading path
R: Radius of smooth specimen
r_D: Polar diameter of the critical domain.

Data Availability

The data are from previously reported studies, and these prior studies are cited at relevant places within the text as references [21, 29–31].

Conflicts of Interest

The authors declare that they have no conflicts of interest.

Acknowledgments

The authors gratefully acknowledge the research support for this work provided by the Scientific Research Start-Up Project of Zhejiang Sci-Tech University (11133132612019) and National Natural Science Foundation of China (52075471).

References

[1] J. F. Barbosa, J. A. Correia, R. Freire Júnior, S.-P. Zhu, and A. M. De Jesus, "Probabilistic S-N fields based on statistical distributions applied to metallic and composite materials: state of the art," *Advances in Mechanical Engineering*, vol. 11, no. 8, p. 168781401987039, 2019.

[2] N. Ottosen, R. Stenström, and M. Ristinmaa, "Continuum approach to high-cycle fatigue modeling," *International Journal of Fatigue*, vol. 30, no. 6, pp. 996–1006, 2008.

[3] M. V. Borodii, "Determination of the non-proportional cyclic hardening coefficient sensitive to the loading amplitude," *Strength of Materials*, vol. 52, no. 6, pp. 919–929, 2021.

[4] A. Nourian-Avval and A. Fatemi, "Variable amplitude fatigue behavior and modeling of cast aluminum," *Fatigue & Fracture of Engineering Materials & Structures*, vol. 44, no. 6, 2021.

[5] C. Ronchei, A. Carpinteri, G. Fortese et al., "Fretting high-cycle fatigue assessment through a multiaxial critical plane-based criterion in conjunction with the Taylor's point method," *Solid State Phenomena*, vol. 258, pp. 217–220, 2017.

[6] I. Milošević, G. Winter, F. Grün et al., "Influence of size effect and stress gradient on the high-cycle fatigue strength of a 1.4542 steel," *Procedia Engineering*, vol. 160, pp. 61–68, 2016.

[7] H.-R. Li, Y. Peng, Y. Liu, and M. Zhang, "Corrected stress field intensity approach based on averaging superior limit of intrinsic damage dissipation work," *Journal of Iron and Steel Research International*, vol. 25, no. 10, pp. 1094–1103, 2018.

[8] C. Wang, D.-G. Shang, and X.-W. Wang, "A new multiaxial high-cycle fatigue criterion based on the critical plane for ductile and brittle materials," *Journal of Materials Engineering and Performance*, vol. 24, no. 2, pp. 816–824, 2015.

[9] X.-W. Wang and D.-G. Shang, "Determination of the critical plane by a weight-function method based on the maximum shear stress plane under multiaxial high-cycle loading," *International Journal of Fatigue*, vol. 90, pp. 36–46, 2016.

[10] Y.-L. Wu, S.-P. Zhu, J.-C. He, D. Liao, and Q. Wang, "Assessment of notch fatigue and size effect using stress field intensity approach," *International Journal of Fatigue*, Article ID 106279, 2021.

[11] G. Qilafku, N. Kadi, J. Dobranski et al., "Fatigue of specimens subjected to combined loading. Role of hydrostatic pressure," *International Journal of Fatigue*, vol. 23, no. 8, pp. 689–701, 2001.

[12] D. Taylor, "Geometrical effects in fatigue: a unifying theoretical model," *International Journal of Fatigue*, vol. 21, no. 5, pp. 413–420, 1999.

[13] Y. Zeng, M. Li, Y. Zhou, and N. Li, "Development of a new method for estimating the fatigue life of notched specimens based on stress field intensity," *Theoretical and Applied Fracture Mechanics*, vol. 104, p. 102339, 2019.

[14] D. S. Paolino and M. P. Cavatorta, "On the application of the stochastic approach in predicting fatigue reliability using Miner's damage rule," *Fatigue & Fracture of Engineering Materials & Structures*, vol. 37, no. 1, pp. 107–117, 2014.

[15] S. B. Zhao, "Study on the accuracy of fatigue life predictions by the generally used damage accumulation theory," *Journal of Mechanical Strength*, vol. 22, no. 3, pp. 206–209, 2000.

[16] S. P. Zhu, Y. Z. Hao, J. A. F. Oliveira Correia, G. Lesiuk, and A. M. P. Jesus, "Nonlinear fatigue damage accumulation and life prediction of metals: a comparative study," *Fatigue & Fracture of Engineering Materials & Structures*, vol. 42, no. 6, pp. 1271–1282, 2019.

[17] Ö. G. Bilir, "Experimental investigation of fatigue damage accumulation in 1100 Al alloy," *International Journal of Fatigue*, vol. 13, no. 1, pp. 3–6, 1991.
[18] P. Kurath, H. Sehitoglu, J. D. Morrow et al., "Effect of selected sub-cycle sequences in fatigue loading histories," *American Society of Mechanical Engineers, Pressure Vessels and Piping Division*, vol. 72, pp. 43–60, 1983.
[19] Y. Wang, D. Zhang, and W. Yao, "Fatigue damage rule of LY12CZ aluminium alloy under sequential biaxial loading," *Science China Physics, Mechanics and Astronomy*, vol. 57, no. 1, pp. 98–103, 2014.
[20] S.-P. Zhu, D. Liao, Q. Liu, J. A. F. O. Correia, and A. M. P. De Jesus, "Nonlinear fatigue damage accumulation: isodamage curve-based model and life prediction aspects," *International Journal of Fatigue*, vol. 128, p. 105185, 2019.
[21] T. X. Xia, W. X. Yao, and L. P. Xu, "Comparative research on accumulative damage models under multiaxial 2-stage step loading spectra for LY12CZ aluminium alloy," *Journal of Aeronautical Materials*, vol. 34, no. 3, pp. 86–92, 2014.
[22] D. Shang and W. X. Yao, "Study on nonlinear continuous damage cumulative model for multiaxial fatigue," *Acta Aeronautica Et Astronautica Sinica*, vol. 19, no. 6, pp. 647–656, 1998.
[23] C. T. Hua, *Fatigue Damage and Small Crack Growth during Biaxial Loading*, University of Illinois, Urbana, IL, USA, 1984.
[24] R. Yuan, H. Li, Z. H. Hong et al., "A new non-linear continuum damage mechanics model for fatigue life prediction under variable loading," *Mechanika*, vol. 19, no. 5, pp. 506–511, 2013.
[25] G. Cheng and A. Plumtree, "A fatigue damage accumulation model based on continuum damage mechanics and ductility exhaustion," *International Journal of Fatigue*, vol. 20, no. 7, pp. 495–501, 1998.
[26] C. Gonçalves, J. A. Araújo, and E. N. Mamiya, "Multiaxial fatigue: a stress based criterion for hard metals," *International Journal of Fatigue*, vol. 27, no. 2, pp. 177–187, 2005.
[27] W. X. Yao, "The prediction of fatigue behaviours by stress field intensity approach," *Acta Mechanica Solida Sinica*, vol. 9, no. 4, pp. 337–349, 1996.
[28] A. Öchsner, *Continuum Damage Mechanics*, Springer, Singapore, Asia, 2016.
[29] L. M. C. André, P. M. Juliana, and J. C. V. Herman, "Fatigue damage accumulation in aluminum 7050-T7451 alloy subjected to block programs loading under step-down sequence," *Procedia Engineering*, vol. 2, pp. 2037–2043, 2010.
[30] Y. L. Wang, "Equivalent-conversion method for estimation of various amplitude fatigue life," *Chinese Journal of Applied Mechanics*, vol. 22, no. 1, pp. 90–94, 2005.
[31] Y. Y. Wang, *Multiaxial Fatigue Behavior and Life Estimation of Metal Materials*, Nanjing University of Aeronautics and Astronautics, Nanjing, China, 2005.
[32] T. Matake, "An explanation on fatigue limit under combined stress," *Bulletin of JSME*, vol. 20, no. 141, pp. 257–263, 1977.
[33] T.-X. Xia and W.-X. Yao, "Comparative research on the accumulative damage rules under multiaxial block loading spectrum for 2024-T4 aluminum alloy," *International Journal of Fatigue*, vol. 48, no. 1, pp. 257–265, 2013.